CSFV proliferation is associated with GBF1 and Rab2

WULONG LIANG, MINPING ZHENG, CHANGLEI BAO and YANMING ZHANG*

College of Veterinary Medicine, Northwest A&F University, Yangling, Shaanxi 712100, People's Republic of China

**Corresponding author (Email, ylzhangym@sohu.com)*

The Golgi apparatus and its resident proteins are utilized and regulated by viruses to facilitate their proliferation. In this study, we investigated *Classical swine fever virus* (CSFV) proliferation when the function of the Golgi was disturbed. Golgi function was disturbed using chemical inhibitors, namely, brefeldin A (BFA) and golgicide A (GCA), and RNA interfering targets, such as the Golgi-specific BFA-resistance guanine nucleotide exchange factor 1 (GBF1) and Rab2 GTPases. CSFV proliferation was significantly inhibited during RNA replication and viral particle generation after BFA and GCA treatment. CSFV multiplication dynamics were retarded in cells transfected with *GBF1* and *Rab2* shRNA. Furthermore, CSFV proliferation was promoted by GBF1 and Rab2 overexpression using a lentiviral system. Hence, Golgi function is important for CSFV multiplication, and GBF1 and Rab2 participate in CSFV proliferation. Further studies must investigate Golgi-resident proteins to elucidate the mechanism underlying CSFV replication.

[Liang W, Zheng M, Bao C and Zhang Y 2017 CSFV proliferation is associated with GBF1 and Rab2. *J. Biosci.* **42** 43–56]

1. Introduction

Classical swine fever (CSF) is a highly contagious disease that affects domestic and wild pigs; it is listed as one of the notifiable swine diseases by the Office International Des Epizooties (OIE) (Lin *et al.* 2014). *Classical swine fever virus* (CSFV), which belongs to the genus *Pestivirus* of the *Flaviviridae* family, is a single-stranded positive-sense RNA virus encoding four structural proteins (C, E^{rns}, E1 and E2) and eight non-structural proteins (N^{pro}, P7, NS2, NS3, NS4A, NS4B, NS5A and NS5B) (Lamp *et al.* 2011). These non-structural proteins participate in self-maturation and replication complex assembly (Sheng *et al.* 2012).

Plus-stranded RNA viruses replicate in the cytoplasm, and their synthesis is associated with cellular membrane structures. Specifically, the endoplasmic reticulum (ER) and Golgi apparatus as well as their resident proteins are used by many viruses to complete one or more stages in their life cycle (Ravindran *et al.* 2016; Wang *et al.* 2016). Anterograde and retrograde trafficking of cargo proteins between the ER and Golgi are mediated by the cytosolic coat protein complex II (COP II) and COP I transport systems, respectively. These systems are regulated by viruses to facilitate their multiplication (Rust *et al.* 2001; Richards *et al.* 2002; Yamayoshi *et al.* 2008). Viruses also regulate two important targets, i.e. Golgi-specific BFA-resistance guanine nucleotide exchange factor 1 (GBF1) and Rab2 GTPases, which are primarily involved in Golgi-to-ER retrograde trafficking (Raj 1961; Wessels *et al.* 2006).

Increasing evidence has shown that CSFV replication relies on cellular membrane structures. CSFV can utilize the membranes of autophagosome-like vesicles to facilitate self-replication (Pei *et al.* 2013). CSFV p7, a viroporin protein in the ER and plasma membrane, modifies membrane permeability (Guo *et al.* 2013; Largo *et al.* 2014). According to our previous study, CSFV NS2 and NS5A proteins localize to the ER and regulate cellular oxidative stress to promote CSFV replication (Tang *et al.* 2010; He *et al.* 2012). However, whether Golgi function and its resident proteins are involved in CSFV replication remains unknown.

In this study, chemical inhibitors, shRNA and lentiviral systems were used to regulate the function of Golgi-resident

Keywords. *Classical swine fever virus*; Golgi-specific BFA-resistance guanine nucleotide exchange factor 1 (GBF1); Rab2 GTPase

DOI: 10.1007/s12038-016-9659-0

Published online: 29 December 2016

proteins. The results of these analyses indicated that GBF1 and Rab2 play important roles in CSFV replication.

2. Materials and methods

2.1 *Cells and virus*

Swine testicle (ST) cells were grown in high-glucose Dulbecco's modified Eagle's medium (DMEM; Gibco, Paisley, UK) containing 10% fetal bovine serum (FBS; HyClone, Logan, UT, USA). The CSFV Shimen strain was purchased from the Control Institute of Veterinary Bio-products and Pharmaceuticals (China) and grown in ST cells. The MOI of CSFV infection in this experiment was set at 10 $TCID_{50}$.

2.2 *Antibodies and chemical inhibitors*

The CSFV polyclonal antibody was collected from Hog Cholera Lapinized Virus (HCLV) inoculated pigs and stored at −20°C. The anti-pig IgG-FITC antibody was purchased from Sigma Aldrich (F1638; St. Louis, MO, USA). Goat anti-GBF1 polyclonal antibody (C-16, sc-27940) was purchased from Santa Cruz Biotechnology (Santa Cruz, CA, USA). Rabbit anti-Rab2 polyclonal antibody (ab154729) was purchased from Abcam (Cambridge, UK). Mouse anti-GAPDH antibody was obtained from GenScript (Piscataway, NJ, USA). The secondary antibodies for Western blotting were HRP-labelled goat anti-rabbit IgG, goat anti-mouse IgG, and rabbit anti-goat IgG (Beyotime, Haimen, China). Brefeldin A (BFA) and golgicide A (GCA) were purchased from Selleck Chemicals (Houston, USA).

2.3 *Cell safe concentration of chemical inhibitors*

An MTT assay was used to test the cytotoxicity of BFA and GCA. Various concentrations of BFA and GCA were added to ST cells, which were plated in 96-well plates at a confluence of about 60%. The cells were then maintained in DMEM with 1% FBS at 37°C in 5% CO_2. After 72 h of incubation, the supernatant was removed. Each well was supplemented with 50 μL of MTT (2 μg/mL) and incubated at 37°C for 4 h. MTT was then removed, and 200 μL of DMSO was added to dissolve the formazan crystals. A microplate reader (Thermo, Waltham, MA, USA) was used to determine light absorbance for each well at 490 nm. Untreated ST cells were used as controls.

2.4 *GBF1and Rab2 shRNA vector construction and cell transfection*

The pGFP-V-RS shRNA plasmid (OriGene Co., Rockville, MD, USA) was used to construct *Rab2* and *GBF1* shRNA interference vectors. For each gene, three pairs of interference fragments were used (table 1), which were synthesized and sequenced by BGI Shenzhen (China). ST cells were transfected with the interference vector when cell confluence reached 70–90%. The transfection operation followed the protocol for the jetPRIME transfection reagent (Polyplus-transfection, Illkirch, France). At 48 h post-transfection, 5 μg/mL puromycin was added to continuously screen positive cells for about 20 days. Scrambled shRNA was constructed and transfected using the same methods.

2.5 *Real-time PCR*

Cellular CSFV, *Rab2* or *GBF1* RNA was tested by relative quantitative PCR. CSFV-infected ST cells with or without inhibitors and cells in which genes silenced were collected. Total RNA was isolated using TRIzol (TaKaRa, Dalian, China) according to the manufacturer's instructions. The RNA concentration was determined using a Nucleic Acid and Protein Analyzer (NanoDrop Technologies, Wilmington, DE, USA) at a wavelength of 260 nm. The PrimeScript™ RT Reagent Kit (TaKaRa) was used for reverse transcription and cDNA synthesis. For real-time PCR, specific oligonucleotide primers (table 2) were used to determine the expression levels of different genes. The reaction was performed with SYBR Premix Ex Taq II (TaKaRa) using the Bio-Rad iQ5 system under the following conditions: pre-degeneration at 95°C for 10 min, followed by 40 cycles of degeneration at 95°C for 10 s, and annealing and extension at 60°C for 30 s. RNA expression in the samples was normalized to that of β-actin. The $2^{-\Delta\Delta CT}$ method was used to analyse the data. The ΔC_T values were calculated as the C_T values of the target gene minus the C_T values of β-actin. *GBF1* and *Rab2* gene expression levels in ST cells or CSFV RNA in ST cells at the earliest time point were selected as comparative references, and so the average ΔC_T values were set as the standard reference for the $-\Delta\Delta C_T$ calculation. Then the $2^{-\Delta\Delta CT}$ values were obtained and histograms were obtained in which the height of the bar for each sample represented the average $2^{-\Delta\Delta CT}$ value.

2.6 *Indirect immunofluorescence assay and viral titration*

CSFV-infected cells at 48 hpi were observed by indirect immunofluorescence assay (IFA). Cell monolayers were fixed with 4% paraformaldehyde for 20 min, following cell penetration with 1% Triton X100 for 10 min. Subsequently,

Table 1. Short hairpin RNA (shRNA) inserts

shRNA	Sequence (5′-3′)
GBF1-shRNA1-S	GATCCCGCTGCTCTTCACAAGGTTACCTCAAGAGGGTAACCTTGTGAAGAGCAGCTTTTTA
GBF1-shRNA1-A	AGCTTAAAAAGCTGCTCTTCACAAGGTTACCCTCTTGAGGTAACCTTGTGAAGAGCAGCGG
GBF1-shRNA2-S	GATCCCGCATGAGAGAGCACCTCAAGTTCAAGAGACTTGAGGTGCTCTCTCATGCTTTTTA
GBF1-shRNA2-A	AGCTTAAAAAGCATGAGAGAGCACCTCAAGTCTCTTGAACTTGAGGTGCTCTCTCATGCGG
GBF1-shRNA3-S	GATCCCGCTCTCAGCAGTGAGTCTATTTCAAGAGAATAGACTCACTGCTGAGAGCTTTTTA
GBF1-shRNA3-A	AGCTTAAAAAGCTCTCAGCAGTGAGTCTATTCTCTTGAAATAGACTCACTGCTGAGAGCGG
Rab2-shRNA1-S	GATCCCGCGACACAGGTGTTGGTAAATTCAAGAGATTTACCAACACCTGTGTCGCTTTTTA
Rab2-shRNA1-A	AGCTTAAAAAGCGACACAGGTGTTGGTAAATCTCTTGAATTTACCAACACCTGTGTCGCGG
Rab2-shRNA2-S	GATCCCGGGCAAGAATCCTTTCGTTCCTCAAGAGGGAACGAAAGGATTCTTGCCCTTTTTA
Rab2-shRNA2-A	AGCTTAAAAAGGGCAAGAATCCTTTCGTTCCCTCTTGAGGAACGAAAGGATTCTTGCCCGG
Rab2-shRNA3-S	GATCCCGCCAGCATTCCAATTCCAACATCAAGAGTGTTGGAATTGGAATGCTGGCTTTTTA
Rab2-shRNA3-A	AGCTTAAAAAGCCAGCATTCCAATTCCAACACTCTTGATGTTGGAATTGGAATGCTGGCGG
Scrambled shRNA-S	GATCCCGATGAAATGGATAGAAGTACATCAAGAGGTGTACTTCTATCCATTTCATCTTTTTA
Scrambled shRNA-A	AGCTTAAAAAGATGAAATGGATAGAAGTACACTCTTGATGTACTTCTATCCATTTCATCGG

5% skim milk was added to the cell monolayer at 4°C for 6 h. The CSFV polyclonal antibody was diluted by 100-fold with PBS and incubated with the cell monolayer at 4°C for 8 h. The FITC anti-pig antibody diluted 200-fold was used for coloration at room temperature for 1 h. The nuclei were stained with DAPI at room temperature for 5 min. Images were observed under an inverted fluorescence microscope (Nikon, Tokyo, Japan). CSFV-infected cell supernatants

Table 2. Primers used in this study

Primers	Sequence (5′-3′)	Use
CSFV-F	GATCCTCATACTGCCCACTTAC	Real-time PCR for detection of CSFV
CSFV-R	GTATACCCCTTCACCAGCTTG	
β actin-F	CAAGGACCTCTACGCCAACAC	Real-time PCR for detection of β actin
β actin-R	TGGAGGCGCGATGATCTT	
GBF1-F	CATGGATTACGTCAATCCCCG	Real-time PCR for detection of GBF1
GBF1-R	GGTCATGTGGGTTGGTAAGGG	
Rab2-F	GCCAGCATTCCAATTCCAAC	Real-time PCR for detection of Rab2
Rab2-R	TCCATGTTCTCGTGCAAAAGC	
pCDH-GBF1-F	CCGGAATTCATGGTGGATAAAAATATTTA CATCATTCA	Amplification of GBF1
pCDH-GBF1-R	ATAAGAATGCGGCCGCTTAGTTGACCTCA GAGGTAGGCATG	
pCDH-Rab2-F	CCGGAATTCATGGCGTACGCCTATCTCTTCA	Amplification of Rab2
pCDH-Rab2-R	ATAAGAATGCGGCCGCTCAACAGCAGCCTCCGCC	

were collected for viral titration. The supernatants were serially diluted from $10^{-1.0}$ to $10^{-10.0}$ and added to ST cells in 96-well plates. At 72 hpi, CSFV infection was observed by IFA. The proportionate distance (PD) and the log lower dilution were calculated according to the Reed–Muench method as follows:

$$\text{PD} = (\%\ \text{next above 50\% positive}) - 50\% \Big/ (\%\ \text{next above 50\% positive}) - (\%\ \text{next below 50\% positive})$$

$$\text{Log lower dilution} = \text{dilution in which position is next above 50\% positive}$$

$$\text{lgTCID}_{50} = \text{PD} \times \text{the difference of logarithmic dilution degrees} + \text{Log lower dilution}$$

2.7 *Western blotting*

Cells were collected and incubated in RIPA lysis buffer (Beyotime) containing the proteinase inhibitor PMSF (Beyotime) for 30 min on ice. A BCA Protein Assay Kit (Beyotime) was used to determine protein concentrations. Equivalent amounts of protein samples were separated by 12% SDS-PAGE and transferred to 0.45-μm PVDF membranes (Millipore, Billerica, MA, USA). Membranes were blocked in TBST containing 5% skim milk powder for 2 h at room temperature. Then, membranes were incubated with a mouse anti-GAPDH antibody or the primary antibodies at the appropriate dilutions according to the instructions overnight at 4°C. Afterwards, the HRP-conjugated secondary antibodies diluted at 1:2000 were added and incubated for 2 h at room temperature. After washing with TBST, immunoreactive bands were detected using luminol chemiluminescence reagents (Pierce) and analysed by Tanon-410 automatically gel imaging system (Shanghai Tianneng, China).

2.8 *Lentivector construction and lentivirus production*

The primers used for *GBF1* and *Rab2* gene amplification contained *Eco*RI and *Not*I restriction sites. The lentivector pCDH-CMV-MCS-EF1-GreenPuro (CD513B-1) (SBI, Mountain View, CA, USA) was used to construct the over-expression vectors pCDH-GBF1 and pCDH-Rab2. The overexpression vector was transfected into HEK-293T cells with three auxiliary plasmids (pGag/Pol, pRev, and pVSV-G). The supernatant of HEK-293T cells was replaced with advanced DMEM contain 2% FBS, 0.01 mM cholesterol, 0.01 mM lecithin, and 1× chemically defined lipid concentrate (Invitrogen, Carlsbad, CA, USA) 16 h post-transfection. The lentiviruses were collected after 48 h post-transfection. ST cells monolayers supplemented with Polybrene at a final concentration of 8 μg/mL and infected using overexpression lentiviruses (MOI=1). The culture medium was replaced with fresh medium at 24 hpi. After another 48 h of incubation, the cells overexpressing *GBF1* and *Rab2* were used for evaluation and subsequent tests.

2.9 *Statistical analysis*

Differences among groups were examined for statistical significance using Student's *t*-tests. $P<0.05$ was considered statistically significant.

3. Results

3.1 *BFA treatment inhibited CSFV proliferation in infected ST cells*

The safe concentration of BFA in ST cells was tested using an MTT assay. The inhibitors were co-cultured with ST cells for 72 h. The concentration of BFA used in the antiviral experiment was 100 nM (figure 1A). After 1 h of CSFV infection, the unbound viruses were removed with the supernatant, and the cells were maintained in media with or without BFA. The cell monolayers were harvested for real-time PCR, and the supernatants were collected for viral titration after 24, 48 and 72 hpi. Cellular CSFV RNA loads decreased by about 2–6 times after BFA treatment (figure 1B). The $TCID_{50}$ of CSFV exhibited a titer reduction of approximately 1.5–2.5 in the BFA treatment group compared with the untreated group (figure 1C). CSFV proliferation with BFA was evaluated by IFA. The CSFV plaques were smaller and less abundant than the untreated ST cells at all three test points (figure 1D).

3.2 *CSFV multiplication was inhibited by GCA*

GCA is a specific inhibitor of GBF1. Before the anti-CSFV test, the cytotoxicity of GCA was detected and, 400 nM was considered the maximum safe concentration for ST cells. This concentration was used in subsequent experiments (figure 2A). GCA cell treatment and the collection of cell monolayers and supernatants were performed using the same methods as those for BFA.

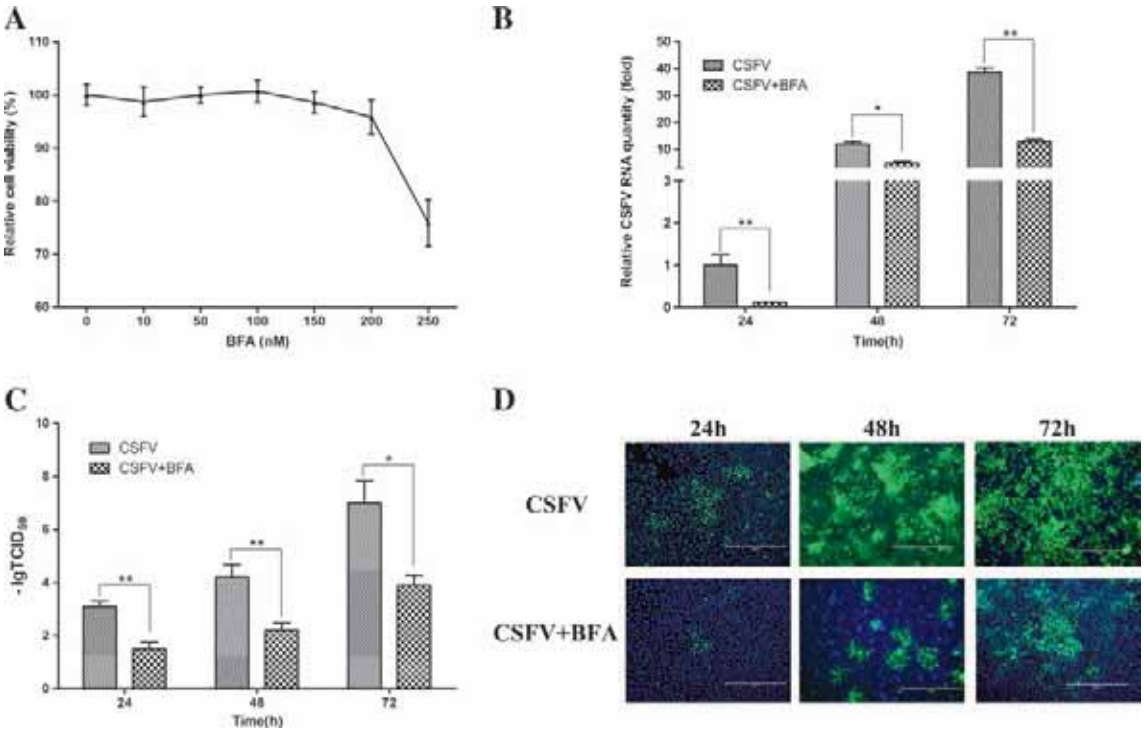

Figure 1. CSFV replication was sensitive to BFA. (**A**) The safe concentration of BFA was tested using an MTT assay. ST cell monolayers in 96-well plates with various concentrations of BFA were cultured for 72 h at 37°C. Relative cell viability was calculated by comparing the $O.D._{490}$ values of BFA-treated cells with those of untreated control cells (set to 100%). (**B**) Cellular CSFV RNA with or without 100 nM BFA were examined by real-time PCR. (**C**) The titers of CSFV with or without BFA were examined by IFA. (**D**) CSFV proliferation in ST cells with or without BFA was observed by IFA at 24, 48 and 72 hpi. Results from three independent experiments are shown as means ± SD. *P<0.05 and **P<0.01 compared with the control group.

Compared with the untreated ST cells, cellular CSFV RNA declined significantly when GCA was added during viral proliferation (figure 2B). Moreover, the viral titer and the percentage of infected ST cells were lower in GCA-treated cells than control cells (figure 2C, D).

3.3 *GBF1 was involved in CSFV replication*

Three shRNA vectors for the swine *GBF1* gene and a scrambled shRNA vector were constructed and transfected into ST cells (figures 3A). After puromycin screening, the down-regulation of *GBF1* in the transfected cells was tested. *GBF1* was knocked down using three shRNA vectors. shRNA-3 was the most effective and was therefore selected for further analysis. Moreover, the transcription levels of the *GBF1* were not significantly different between the untransfected cells and scrambled shRNA-transfected cells (figure 3B, C). The CSFV proliferation dynamics in ST cells, *GBF1* shRNA -transfected cells, and scrambled shRNA-transfected cells were then evaluated. CSFV was incubated with cell monolayers at 37°C for 1 h, and unbound particles were removed with the supernatants. Infected cell monolayers were collected for CSFV RNA quantitative detection, and the supernatants were collected for viral titration at 24, 48 and 72 hpi. The detection of cellular CSFV RNA and viral titers showed that the CSFV proliferation dynamics in *GBF1* shRNA-transfected cells were slower than those in ST cells and scrambled shRNA-transfected cells (figure 4A, B). CSFV proliferation in ST cells, *GBF1* shRNA-transfected cells, and scrambled shRNA-transfected cells was observed by IFA. The percentage of CSFV-infected GBF1 knockdown cells was significantly lower than those of the infected ST cells and scrambled shRNA-transfected cells, especially at 48 and 72 hpi. GFP expression in shRNA-transfected cells was quenched after fixation with 4% paraformaldehyde, which had no effect on the observation of FITC on anti-pig IgG (figure 4C).

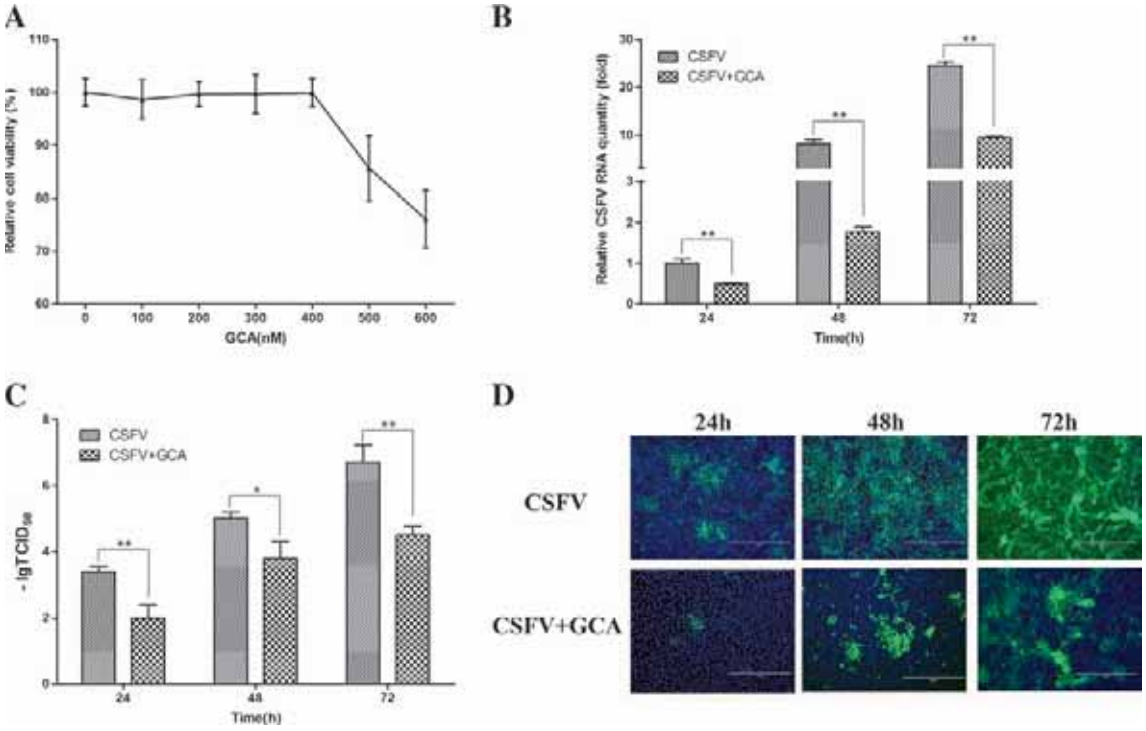

Figure 2. CSFV multiplication was inhibited by GCA. (**A**) The safe concentration of GCA was tested using the MTT assay. The operations and calculations were the same as those used for BFA. (**B**) Cellular CSFV RNA with or without 400 nM GCA were examined using real-time PCR. (**C**) The titers of CSFV with or without GCA were tested by IFA. (**D**) CSFV proliferation in ST cells with or without GCA was observed by IFA at 24, 48 and 72 hpi. Results from the three independent experiments are shown as means ± SD. *P<0.05 and **P<0.01 compared with the control group.

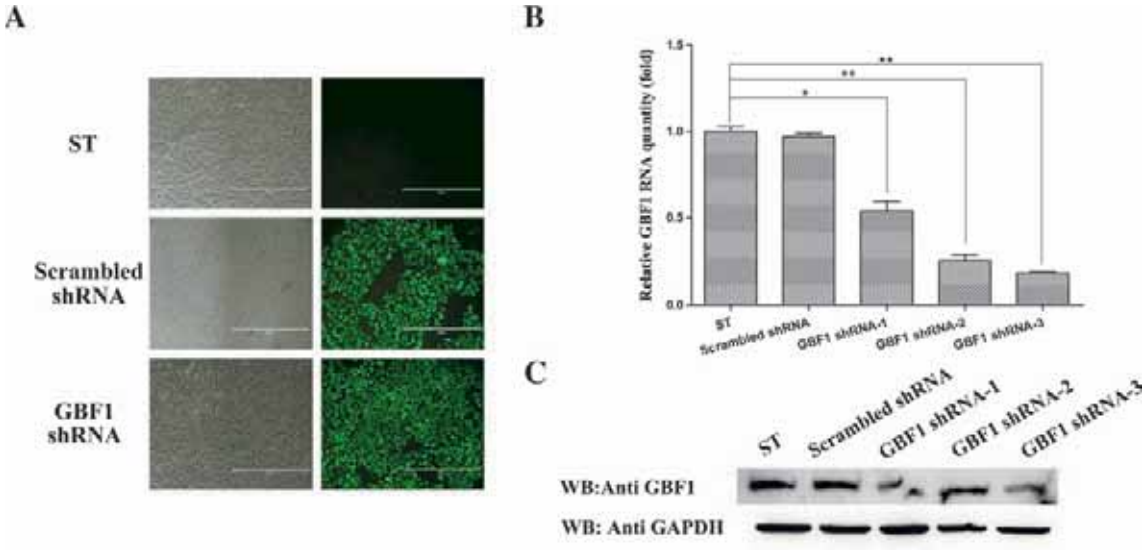

Figure 3. Construction and selection of cells with down-regulated GBF1. (**A**) ST cells transfected with scrambled shRNA or *GBF1* shRNA were selected by adding 5 μg/mL puromycin for about 20 days (only *GBF1* shRNA-3 transfected cells are shown). (**B**) *GBF1* RNA transcription in ST cells, scrambled shRNA, and *GBF1* shRNA-transfected cells were examined by real-time PCR. (**C**) GBF1 protein in ST cells, scrambled shRNA, and GBF1 shRNA-transfected cells were examined by Western blotting. Results from the three independent experiments are shown as means ± SD. *P<0.05 and **P<0.01 compared with the control group.

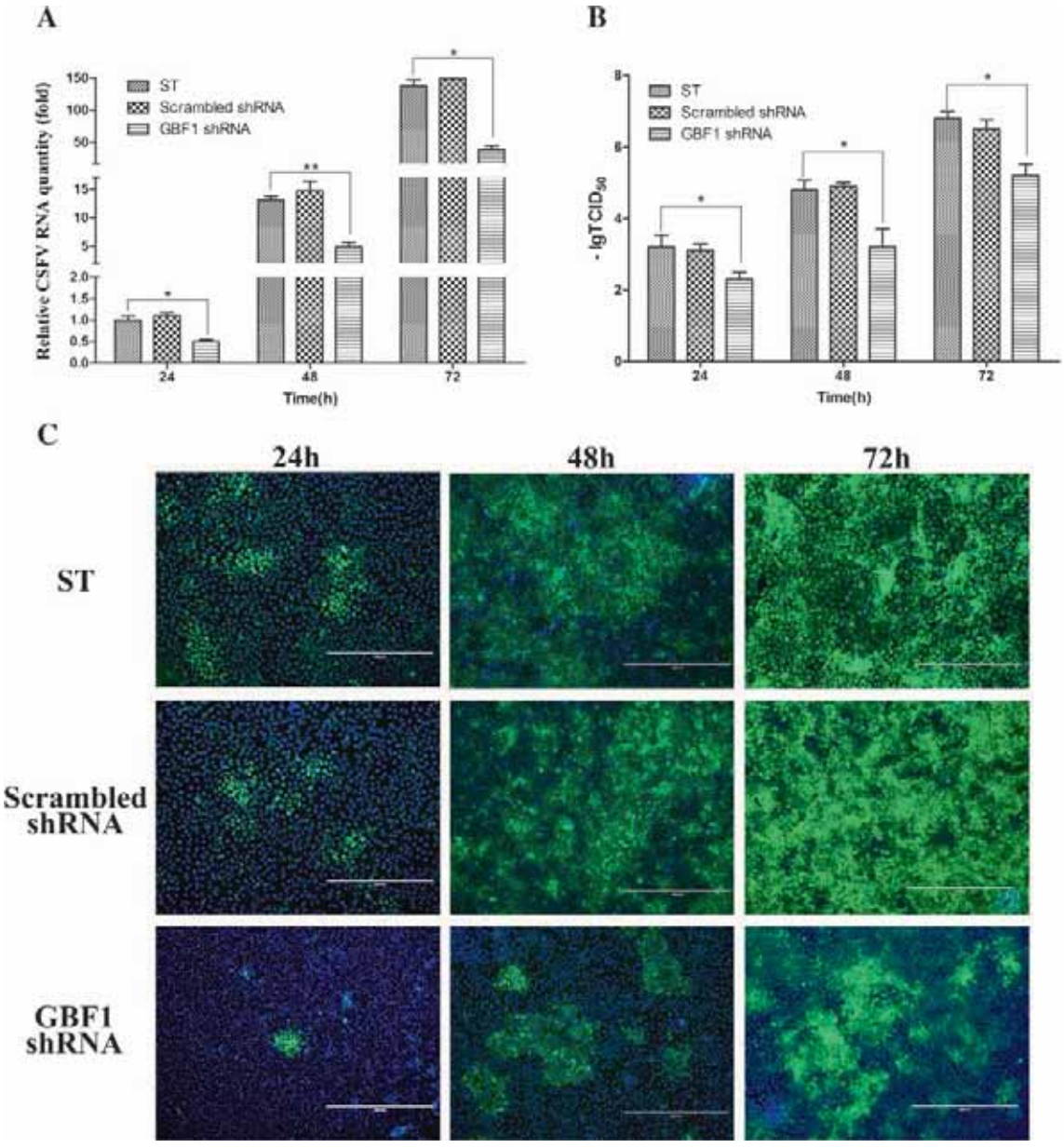

Figure 4. CSFV proliferation dynamic in GBF1 knockdown cells. (**A**) CSFV proliferation dynamics in ST cells, scrambled shRNA-transfected cells, and *GBF1* shRNA-transfected cells were examined by real-time PCR. (**B**) CSFV titers in ST cells, scrambled shRNA-transfected cells, and *GBF1* shRNA-transfected cells were examined by IFA. (**C**) CSFV proliferation in ST cells, scrambled shRNA-transfected cells, and GBF1 shRNA-transfected cells observed by IFA at 24, 48 and 72 hpi. Results from the three independent experiments are shown as means ± SD. *P<0.05 and **P<0.01 compared with the control group.

3.4 *CSFV proliferation required the assistance of Rab2*

shRNA vectors and transfected cells specific to the swine *Rab2* gene were constructed and selected using the same methods used for the *GBF1* gene. *Rab2* shRNA-1 demonstrated the optimal down-regulation of expression (figure 5B, C), and the corresponding transfected cells were used for the anti-CSFV test. Cellular CSFV RNA tested by real-time PCR at three time points showed that the down-regulation of the *Rab2* gene significantly slowed CSFV RNA replication. Cellular CSFV RNA in *Rab2* knockdown cells declined by about 10 times relative to

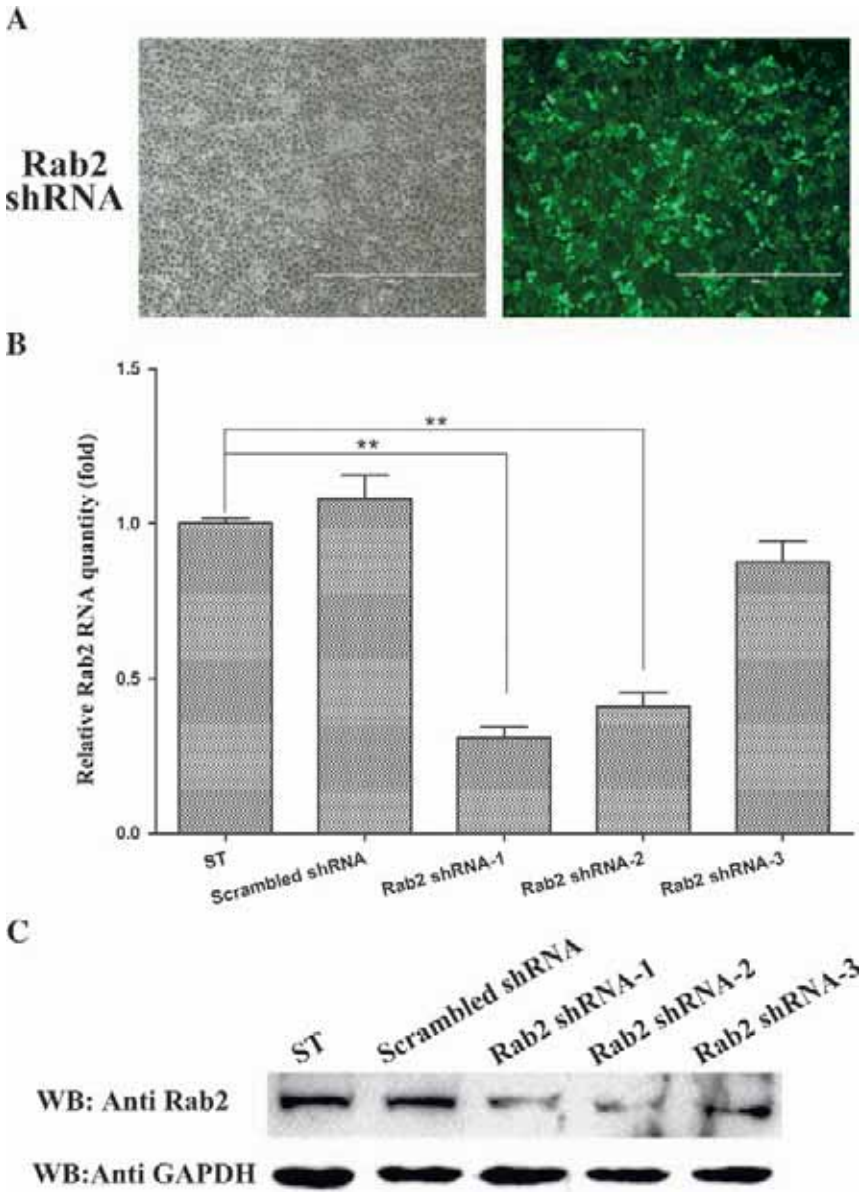

Figure 5. Construction and selection of cells with downregulated *Rab2*. (**A**) *Rab2* shRNA was stably transfected to ST cells (only *Rab2* shRNA-1-transfected cell are shown). (**B**) Relative expression of *Rab2* in ST cells and scrambled shRNA- or *Rab2* shRNA-transfected cells were examined using real-time PCR. (**C**) Rab2 protein levels in ST cells, scrambled shRNA-transfected cells, and *GBF1* shRNA-transfected cells were analysed by Western blotting. Results from the three independent experiments are shown as means ± SD. *P<0.05 and **P<0.01 compared with the control group.

the levels in ST cells and scrambled shRNA-transfected cells (figure 6A). In addition, viral titration showed that the production of CSFV virions declined by about 1–2.5 titers by *Rab2* knock-down (figure 6B). Furthermore, CSFV-infected *Rab2* interference cells were less abundant than cells of the control groups at the three testing points (figure 6C).

3.5 *GBF1 and Rab2 overexpression facilitated CSFV proliferation*

GBF1 and *Rab2* were overexpressed using the lentiviral vector system. *GBF1* and *Rab2* expression increased at both the mRNA (figure 7B, C) and protein levels (figure 7D, E). CSFV proliferation was higher after the upregulation of

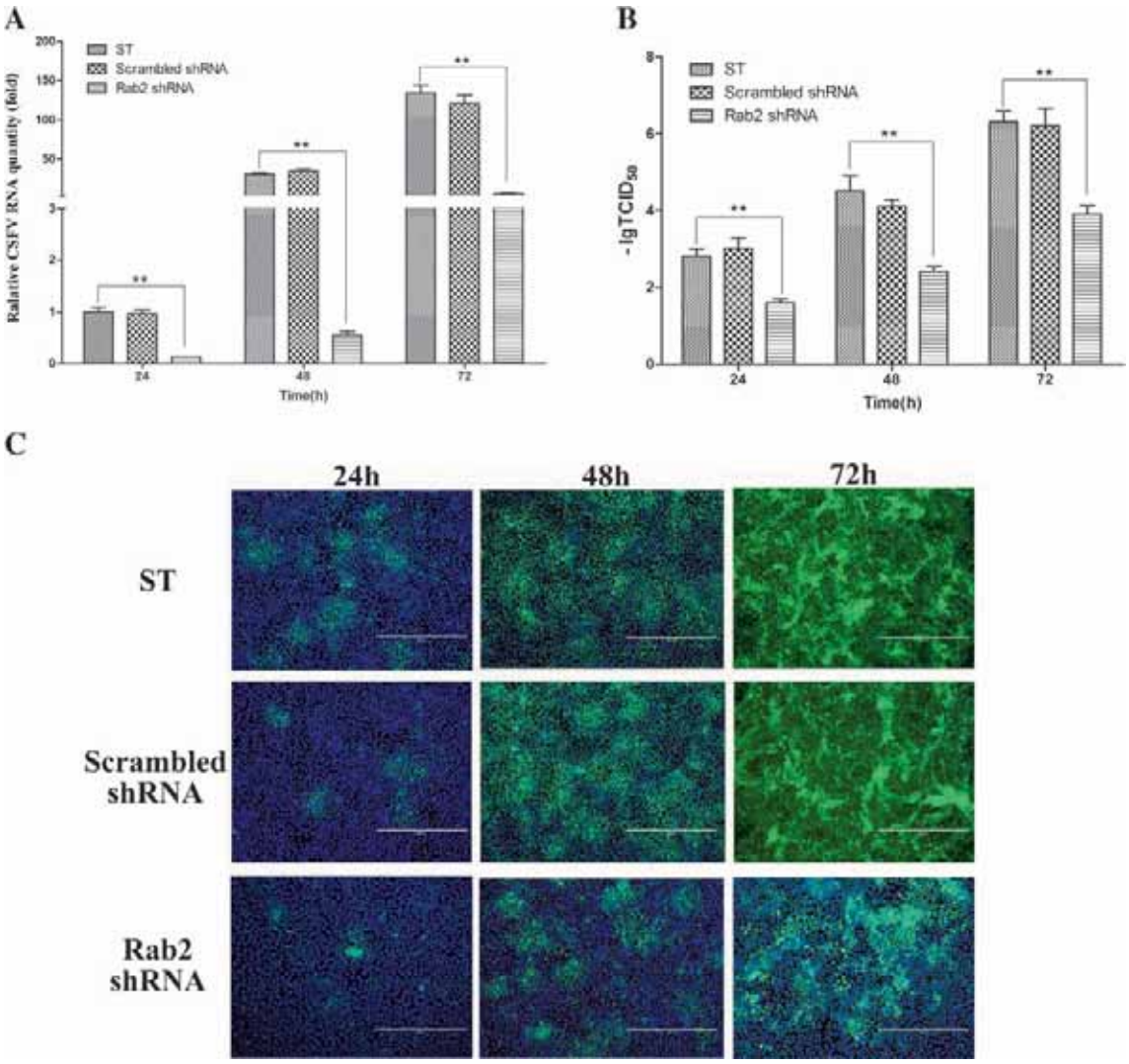

Figure 6. CSFV proliferation dynamic in Rab2 knockdown cells. (**A**) CSFV proliferation dynamics in ST cells, scrambled shRNA-transfected cells, and *Rab2* shRNA-transfected cells were examined by real-time PCR. (**B**) CSFV titers in ST cells, scrambled shRNA-transfected cells, and *Rab2* shRNA-transfected cells were examined by IFA. (**C**) CSFV proliferation in ST cells, scrambled shRNA-, and *Rab2* shRNA-transfected cells observed by IFA at 24, 48 and 72 hpi. Results from the three independent experiments are shown as means ± SD. *P<0.05 and **P<0.01 compared with the control group.

GBF1 and *Rab2* compared with ST cells and the mock lentivirus group (figure 8).

3.6 *GBF1 and Rab2 regulated CSFV RNA replication*

Cellular CSFV RNA in the first 12 h was measured by real-time PCR to evaluate whether *GBF1* and *Rab2* regulate CSFV RNA replication. CSFV RNA replication was suppressed when *GBF1* and *Rab2* were disturbed by inhibitors or shRNA (figure 9A, B). Conversely, overexpression of *GBF1* and *Rab2* could accelerate CSFV RNA replication (figure 9C).

4. Discussion

The functions of CSFV non-structural proteins have been studied extensively in recent years (Lamp *et al.* 2011; Sheng *et al.* 2012); nevertheless, the CSFV replication mechanism and the subcellular location of the replication complex remain unclear. Studies on the replication membranes of positive-stranded viruses demonstrated that they

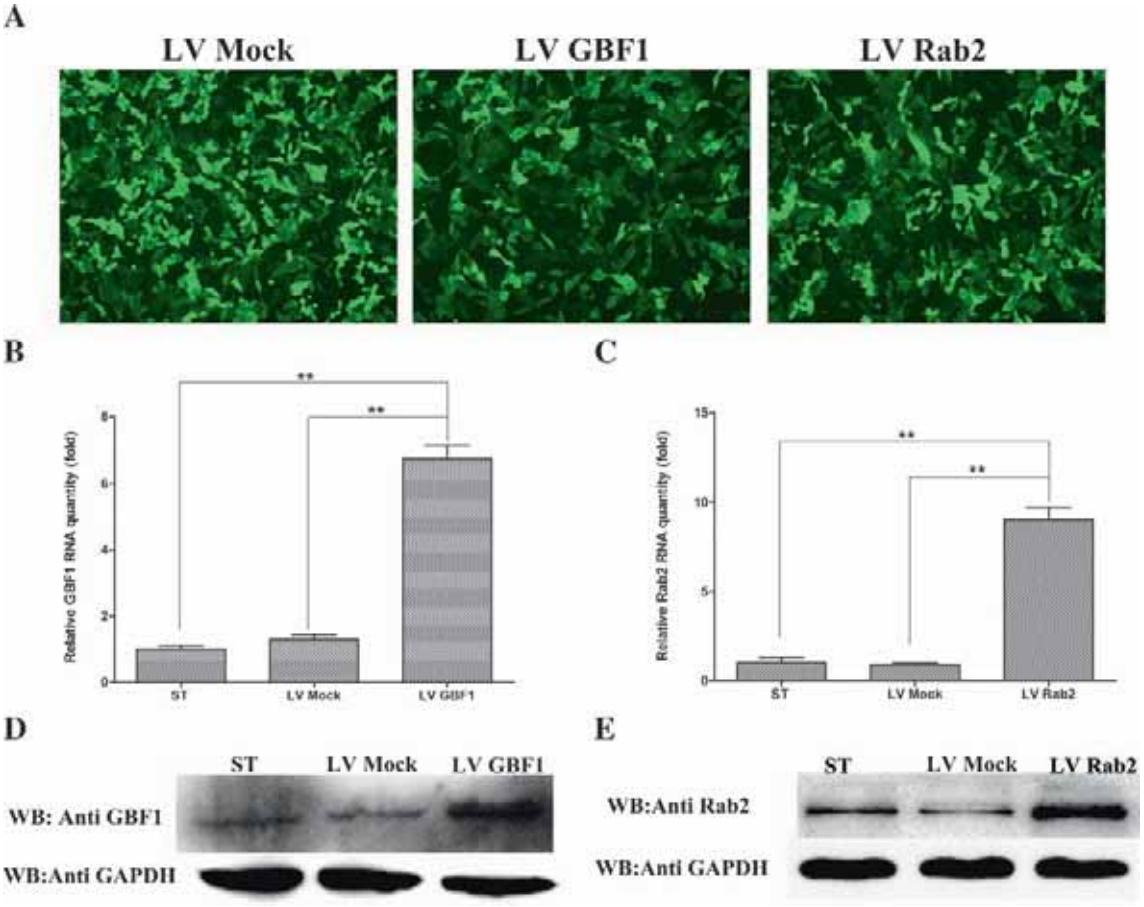

Figure 7. Overexpression of *GBF1* and *Rab2* using a lentivirus (LV) system. (**A**) Fluorescent photographs of ST cells infected with lentiviruses. LV Mock: lentivirus without exogenous gene, LV GNF1: lentivirus carrying the *GBF1* gene, LV Rab2: lentivirus carrying the *Rab2* gene. (**B**–**C**) Overexpression of *GBF1* or *Rab2* was evaluated by real-time PCR. (**D**–**E**) Overexpression of *GBF1* or *Rab2* was evaluated by western blotting. Results from the three independent experiments are shown as means ± SD. *P<0.05 and **P<0.01 compared with the control group.

can induce the alteration of intracellular membranes to facilitate the replication cycle (Miller and Krijnse-Locker 2008). CSFV NS2 and NS5A are located in the ER (Tang *et al.* 2010; He *et al.* 2012). NS5B, which is an RNA-dependent RNA polymerase of CSFV, is located in the cytoplasm (Zhao *et al.* 2006). The locations of these CSFV replication-associated proteins suggest that the complex is located in the cytoplasm, and the ER may support CSFV replication. However, it is not clear whether other intracytoplasmic membrane structures and their resident proteins are involved in CSFV replication.

In this study, we found that CSFV replication is sensitive to BFA. Both CSFV RNA replication and virus particle generation were inhibited by BFA treatment. BFA inhibited protein transport between the ER and the Golgi by suppressing the formation of COP I-mediated transport vesicles. The proliferation of viruses, such as hepatitis C virus (HCV) (Goueslain *et al.* 2010) and dengue virus (Carpp *et al.* 2014), is sensitive to BFA treatment owing to the inhibitory effect of BFA on GBF1 and the consequent inhibition of COP I vesicle formation. However, three BFA-sensitive large Arf-GEFs (GBF1, BIG1 and BIG2) are present in mammalian cells (Li *et al.* 2014). Therefore, GCA and RNA interference were used for further tests. GCA is a highly specific inhibitor of GBF1 and had the same inhibitory effect on CSFV proliferation as BFA. Furthermore, CSFV replication in *GBF1* shRNA-transfected cells was significantly inhibited compared with that in *GBF1*-undisturbed cells. Conversely, CSFV multiplication was increased in cells overexpressing *GBF1*. Therefore, GBF1 participated in CSFV multiplication.

GBF1 participates in the retrograde Golgi-to-ER transportation by activating the ADP-ribosylation factor (ARF) to regulate cytosolic COP I recruitment (Zhao *et al.* 2006;

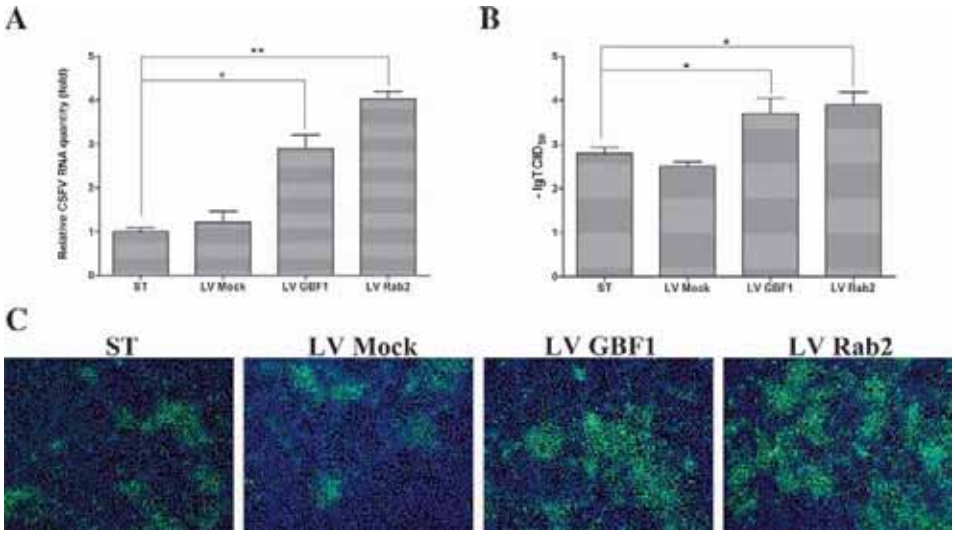

Figure 8. CSFV proliferation was accelerated by the overexpression of GBF1 and Rab2. (**A**) CSFV proliferation dynamics in ST cells and LV Mock, LV GBF1, and LV Rab2 infected cells were evaluated by real-time PCR at 24 hpi. (**B**) CSFV titers in ST cells and LV Mock, LV GBF1, and LV Rab2 infected cells were examined by IFA at 24 hpi. (**C**) CSFV proliferation in ST cells and LV Mock, LV GBF1, and LV Rab2 infected cells were observed by IFA at 24 hpi. Results from the three independent experiments are shown as means ± SD. *P<0.05 and **P<0.01 compared with the control group.

Lowery *et al.* 2013). GBF1 is involved in the multiplication of many viruses, such as severe acute respiratory syndrome coronavirus (SARS-CoV) (de Wilde *et al.* 2015), dengue virus (Carpp *et al.* 2014) and influenza virus (Watanabe *et al.* 2014). One of the mechanisms by which GBF1 regulates viral multiplication involves the GBF1-ARF1-COP I pathway. HCV replication is suppressed when the functions of GBF1 and ARF1 are disturbed (Goueslain *et al.* 2010; Matto *et al.* 2011). Dengue virus uses the GBF1-ARF1/ARF4-COP I pathway to form capsids around lipid droplets (Iglesias *et al.* 2015). GBF1-mediated ARF1 activation is crucial for mouse hepatitis coronavirus (MHV) RNA replication (Verheije *et al.* 2008), Ebola virus virion formation (Yamayoshi *et al.* 2010), and diverse families of negative-stranded RNA viruses (Panda *et al.* 2011). Other metabolic pathways are also regulated by GBF1 and are involved in virus proliferation. GBF1 simultaneously regulates ARF4 and ARF5 to modulate HCV replication (Farhat *et al.* 2016). GBF1 has other functions in HCV replication in BFA-resistant hepatoma-derived cells (Farhat *et al.* 2012). Here, we discovered that both CSFV RNA replication and virus particle formation were inhibited by the disturbance of GBF1 function. However, the CSFV proliferation dynamics in *ARF1* shRNA-transfected cells were not different from those in control cells (data not shown). Therefore, GBF1 may regulate some metabolic pathways without ARF1 to modulate CSFV proliferation. The detailed function of GBF1 in CSFV proliferation requires further investigation.

Rab2 is a component of pre-Golgi intermediates that mainly regulates retrograde trafficking from the ERGIC (ER-Golgi intermediate compartment) to the ER (Ortiz Sandoval and Simmen 2012). Moreover, Rab2 is essential for Golgi organization (Haas *et al.* 2007) and can regulate COP I-mediated retrograde transport to intervene with the release of HCV particles (Raj 1961). In the present study, CSFV replication was suppressed when Rab2 was down-regulated. The overexpression of Rab2 can accelerate CSFV proliferation. The mechanisms by which Rab2 influences CSFV proliferation must be further investigated.

As the cargo sorting station within the cell, the Golgi apparatus participates in protein and vesicular transport (Mironov *et al.* 2013; Guo *et al.* 2014). Additionally, the secretory pathways involved in the Golgi apparatus are always utilized by viruses for egress on infected cells. Transport from early endosomes to the trans-Golgi network is important for vaccinia virus membrane wrapping and egress (Sivan *et al*. 2016). Human herpesvirus-6 (HHV-6) can egress via the exosomal release pathway by budding at trans-Golgi network vacuoles and inducing multivesicular body formation (Mori *et al*. 2008). Furthermore, the hepatitis E virus and HCV also utilize the exosome release pathway for egress (Tamai *et al*. 2011; Nagashima *et al*. 2014). However, viral egress is a complicated process that involves many pathways and related proteins. Reports have shown that HCV can be released from Huh7 cells via a trans-Golgi network-to-endosome pathway (Jamel *et al*. 2016).

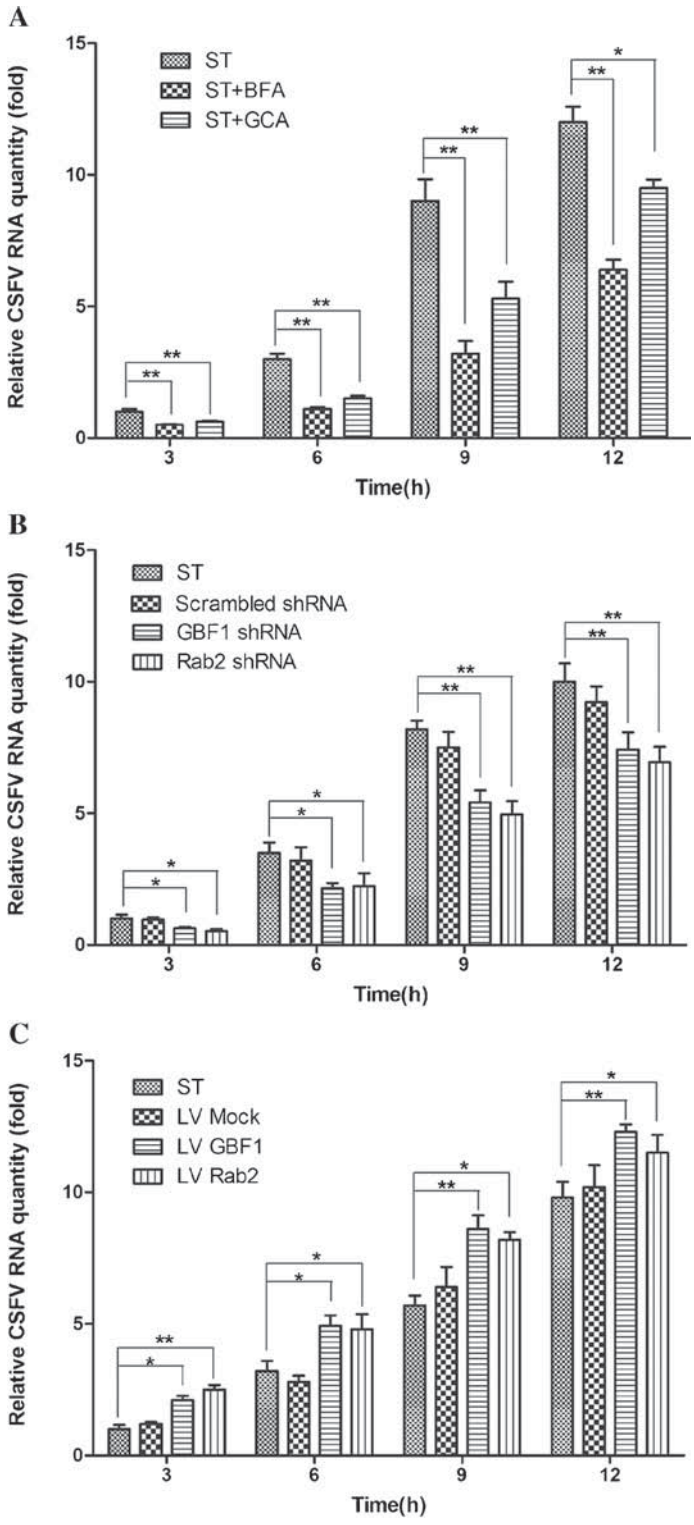

Figure 9. GBF1 and Rab2 regulated CSFV RNA replication. (**A**) CSFV replication with or without BFA and GCA was tested by real-time PCR at 3, 6, 9 and 12 hpi. (**B**) CSFV replication in ST cells, scrambled shRNA-transfected cells, *GBF1* shRNA-transfected cells, and *Rab2* shRNA-transfected cells were examined by real-time PCR at 3, 6, 9 and 12 hpi. (**C**) CSFV replication in ST cells and LV Mock, LV GBF1 and LV Rab2 infected cells were evaluated by real-time PCR at 3, 6, 9 and 12 hpi. Results from three independent experiments are shown as means ± SD. *P<0.05 and **P<0.01 compared with the control group.

Additionally, HCV particles are found in endosomal compartments and released via a non-canonical secretory route that is unrelated to the Golgi-associated secretory route and may be an undescribed cellular secretion route (Bayer *et al*. 2016). Viral egress has a close connection with the virus particle formation process. CSFV is a single-stranded positive-sense RNA virus that has no cytopathic effect in infected cells. The CSFV assembly process is still unclear and mysterious because its core protein is dispensable for CSFV assembly (Riedel *et al.* 2012). Additional experiments are urgently needed to determine the mechanisms of CSFV assembly and egress.

In summary, we demonstrated that *GBF1* and *Rab2* play important roles in CSFV proliferation. Golgi and pre-Golgi intermediates are also important in CSFV replication. Nevertheless, the effect of COP I-mediated retrograde trafficking on CSFV replication must be further investigated.

Acknowledgements

This work was supported by the National Natural Science Foundation of China (No. 31472210).

References

Bayer K, Banning C, Bruss V, Wiltzer-Bach L and Schindler M 2016 Hepatitis c virus is released via a non-canonical secretory route. *J. Virol.* **14** 10558–10573

Carpp LN, Rogers RS, Moritz RL and Aitchison JD 2014 Quantitative proteomic analysis of host-virus interactions reveals a role for Golgi brefeldin A resistance factor 1 (GBF1) in dengue infection. *Mol. Cell. Proteomics* **13** 2836–2854

de Wilde AH, Wannee KF, Scholte FE, Goeman JJ, Ten DP, Snijder EJ, Kikkert M and van Hemert MJ 2015 A Kinome-wide small interfering RNA screen identifies proviral and antiviral host factors in severe acute respiratory syndrome coronavirus replication, including double-stranded RNA-activated protein kinase and early secretory pathway proteins. *J. Virol.* **89** 8318–8333

Farhat R, Goueslain L, Wychowski C, Belouzard S, Fénéant L, Jackson CL, Dubuisson J and Rouillé Y 2012 Hepatitis C virus replication and Golgi function in brefeldin a-resistant hepatoma-derived cells. *PLoS One* **8** 454

Farhat R, Séron K, Ferlin J, Fénéant L, Belouzard S, Goueslain L, Jackson CL, Dubuisson J, et al 2016 Identification of class II ADP-ribosylation factors as cellular factors required for hepatitis C virus replication. *Cell Microbiol.* **27**. doi:10.1111/cmi.12572

Goueslain L, Alsaleh K, Horellou P, Roingeard P, Descamps V, Duverlie G, Ciczora Y, Wychowski C, *et al*. 2010 Identification of GBF1 as a cellular factor required for hepatitis C virus RNA replication. *J. Virol.* **84** 773–787

Guo HC, Sun SQ, Sun DH, Wei YQ, Xu J, Huang M, Liu XT, Liu ZX, *et al*. 2013 Viroporin activity and membrane topology of classic swine fever virus p7 protein. *Int. J. Biochem. Cell Biol.* **45** 1186–1194

Guo Y, Sirkis DW and Schekman R 2014 Protein sorting at the trans-golgi network. *Annu. Rev. Cell Dev. Biol.* **30** 169–206

Haas AK, Yoshimura S, Stephens DJ, Preisinger C, Fuchs E and Barr FA 2007 Analysis of GTPase-activating proteins: Rab1 and Rab43 are key Rabs required to maintain a functional Golgi complex in human cells. *J. Cell Sci.* **120** 2997–3010

He L, Zhang YM, Lin Z, Li WW, Wang J and Li HL 2012 Classical swine fever virus NS5A protein localizes to endoplasmic reticulum and induces oxidative stress in vascular endothelial cells. *Virus Genes.* **45** 274–282

Iglesias NG, Mondotte JA, Byk LA, De Maio FA, Samsa MM, Alvarez C and Gamarnik AV 2015 Dengue virus uses a non-canonical function of the host GBF1-Arf-COPI system for capsid protein accumulation on lipid droplets. *Traffic* **16** 962–977

Jamel M, Cheryl W, Hazel S, Matthew B, Sun PW, Do HW, Mitsunori F, Stephen G, *et al*. 2016 Release of infectious hepatitis c virus from huh7 cells occurs via atrans-golgi network-to-endosome pathway independent of very-low-density lipoprotein secretion. *J. Virol.* **90** 7159–7170

Lamp B, Riedel C, Roman-Sosa G, Heimann M, Jacobi S, Becher P, Thiel HJ and Rümenapf T 2011 Biosynthesis of *Classical Swine Fever Virus* nonstructural proteins. *J. Virol.* **85** 3607–3620

Largo E, Gladue DP, Huarte N, Borca MV and Nieva JL 2014 Pore-forming activity of pestivirus p7 in a minimal model system supports genus-specific viroporin function. *Antivir. Res.* **101** 30–36

Li C, Chen S, Yu Y, Zhou C, Wang Y, Le K, Li D, Shao W, *et al*. 2014 BIG1, a brefeldin A-inhibited guanine nucleotide-exchange factor, is required for GABA-Gated Cl – influx through regulation of GABA a receptor trafficking. *Mol. Neurobiol.* **49** 808–819

Lin Z, Liang W, Kang K, Li H, Cao Z and Zhang Y 2014 Classical swine fever virus and p7 protein induce secretion of IL-1β in macrophages. *J. Gen. Virol.* **95** 2693–2699

Lowery J, Szul T, Styers M, Holloway Z, Oorschot V, Klumperman J and Sztul E 2013 The Sec7 guanine nucleotide exchange factor GBF1 regulates membrane recruitment of BIG1 and BIG2 guanine nucleotide exchange factors to the Trans-Golgi Network (TGN). *J. Biol. Chem.* **288** 11532–11545

Matto M, Sklan EH, David N, Melamed-Book N, Casanova JE, Glenn JS and Aroeti B 2011 Role for ADP ribosylation factor 1 in the regulation of hepatitis C virus replication. *J. Virol.* **85** 946–956

Miller S and Krijnse-Locker J 2008 Modification of intracellular membrane structures for virus replication. *Nat. Rev. Microbiol.* **6** 363–374

Mironov AA, Sesorova IV and Beznoussenko GV 2013 Golgi's way: a long path toward the new paradigm of the intra-golgi transport. *Histochem. Cell Biol.* **140** 383–393

Mori Y, Koike M, Moriishi E, Moriishi A, Kawabata H, Tang H, Oyaizu YU, *et al*. 2008 Human herpesvirus-6 induces mvb formation, and virus egress occurs by an exosomal release pathway. *Traffic.* **9** 1728–1742

Nagashima S, Jirintai S, Takahashi M, Kobayashi T, Tanggis NT, Kouki T, Yashiro T, *et al*. 2014 Hepatitis e virus egress depends on the exosomal pathway, with secretory exosomes derived from multivesicular bodies. *J. Gen. Virol.* **95** 2166–2175

Ortiz Sandoval C and Simmen T 2012 Rab proteins of the endoplasmic reticulum: functions and interactors. *Biochem. Soc. Trans.* **40** 1426–1432

Panda D, Das A, Dinh PX, Subramaniam S, Nayak D, Barrows NJ, Pearson JL, Thompson J, *et al*. 2011 RNAi screening reveals requirement for host cell secretory pathway in infection by diverse families of negative-strand RNA viruses. *Proc. Natl. Acad. Sci. USA* **108** 19036–19041

Pei J, Zhao M, Ye Z, Gou H, Wang J, Yi L, Dong X, Liu W, *et al*. 2013 Research article: autophagy enhances the replication of classical swine fever virus in vitro. *Autophagy* **10** 93–110

Raj M 1961 Biological roles of cellular glyceraldehyde-3-phosphate dehydrogenase in the hepatitis C virus life cycle (University of British Columbia)

Ravindran MS, Bagchi P, Cunningham CN and Tsai B 2016 Opportunistic intruders: how viruses orchestrate ER functions to infect cells. *Nat. Rev. Microbiol.* **14** 407–420

Richards AA, Stang E, Pepperkok R and Parton RG 2002 Inhibitors of COP-mediated transport and cholera toxin action inhibit simian virus 40 infection. *Mol. Biol. Cell* **13** 1750–1764

Riedel C, Lamp B, Heimann M, König M, Blome S, Moennig V, Schüttler C, Thiel HJ, *et al*. 2012 The core protein of classical swine fever virus is dispensable for virus propagation in vitro. *PLoS Pathog.* **8** e1002598

Rust RC, Landmann L, Gosert R, Tang BL, Hong W, Hauri HP, Egger D and Bienz K 2001 Cellular COPII proteins are involved in production of the vesicles that form the poliovirus replication complex. *J. Virol.* **75** 9808–9818

Sheng C, Wang J, Xiao J, Xiao J, Chen Y, Jia L, Zhi Y, Li G, *et al*. 2012 Classical swine fever virus NS5B protein suppresses the inhibitory effect of NS5A on viral translation by binding to NS5A. *J. Gen. Virol.* **93** 939–950

Sivan G, Weisberg AS, Americo JL and Moss B 2016 Retrograde transport from early endosomes to the trans-golgi network enables membrane wrapping and egress of vaccinia virus virions. *J. Virol.* **90** 8891–8905

Tamai K, Shiina M, Tanaka N, Nakano T, Yamamoto A, Kondo Y, Kakazu E, Inoue J, *et al*. 2011 Regulation of hepatitis c virus secretion by the hrs-dependent exosomal pathway. *Virology.* **422** 377–385

Tang QH, Zhang YM, Fan L, Tong G, He L and Dai C 2010 Classic swine fever virus NS2 protein leads to the induction of cell cycle arrest at S-phase and endoplasmic reticulum stress. *Virol. J.* **7** 1–12

Verheije MH, Raaben M, Mari M, Te Lintelo EG, Reggiori F, van Kuppeveld FJ, Rottier PJ and de Haan CA 2008 Mouse hepatitis coronavirus RNA replication depends on GBF1-mediated ARF1 activation. *PLoS Pathog.* **4** e1000088

Wang RY, Wu YJ, Chen HS and Chen CJ 2016 A KDEL retrieval system for ER-golgi transport of japanese encephalitis viral particles. *Viruses* doi:10.3390/v8020044

Watanabe T, Kawakami E, Shoemaker JE, Lopes TJ, Matsuoka Y, Tomita Y, Kozuka-Hata H, Gorai T, *et al*. 2014 Influenza virus-host interactome screen as a platform for antiviral drug development. *Cell Host Microbe* **16** 795–805

Wessels E, Duijsings D, Niu TK, Neumann S, Oorschot VM, de Lange F, Lanke KH, Klumperman J, *et al*. 2006 A viral protein that blocks Arf1-mediated COP-I assembly by inhibiting the guanine nucleotide exchange factor GBF1. *Dev. Cell* **11** 191–201

Yamayoshi S, Noda T, Ebihara H, Goto H, Morikawa Y, Lukashevich IS, Neumann G, Feldmann H, *et al*. 2008 Ebola virus matrix protein VP40 uses the COPII transport system for its intracellular transport. *Cell Host Microbe* **3** 168–177

Yamayoshi S, Neumann G and Kawaoka Y 2010 Role of the GTPase Rab1b in ebolavirus particle formation. *J. Virol.* **84** 4816–4820

Zhao X, Claude A, Chun J, Shields DJ, Presley JF and Melançon P 2006 GBF1, a cis-Golgi and VTCs-localized ARF-GEF, is implicated in ER-to-Golgi protein traffic. *J. Cell Sci.* **119** 3743–3753

MS received 10 August 2016; accepted 01 December 2016

Corresponding editor: Veena K Parnaik